RSC Advances

PAPER

Cite this: *RSC Adv.*, 2023, **13**, 27764

Organocatalyzed ring-opening reactions of γ-carbonyl-substituted ε-caprolactones†

Takayuki Ota,‡[a] Valentina Montagna,‡[bc] Yuji Higuchi,[d] Takashi Kato,[e] Masaru Tanaka,[f] Haritz Sardon[c] and Kazuki Fukushima *[beg]

Side-chain-functionalized aliphatic polyesters are promising as functional biodegradable polymers. We have investigated ring-opening reactions of γ-carbonyl-substituted ε-caprolactones (gCCLs) to obtain poly(ε-caprolactone) (PCL) analogues. Organic catalysts and $Sn(Oct)_2$ often used for the ring-opening polymerization (ROP) of ε-caprolactone (CL) have been explored to find the conditions for the formation of polymeric products of gCCLs. We confirmed the consumption of gCCLs in all catalyzed reactions. However, chain propagation hardly occurs, as the propagating species are preferentially transformed to α-substituted five-membered lactones when the substituents are linked by ester or not sterically hindered. Intramolecular cyclization to form thermodynamically stable five-membered lactones releases alcohols and amines, serving as nucleophiles for the subsequent ring opening of other gCCLs. Thus, apparent chain reactions are realized for continuous consumption of gCCLs. The reaction preference remains unchanged independent of the catalysts, although the reactions of the amide-linked gCCLs by acidic catalysts are slightly mitigated. Finally, copolymerization of CL and a gCCL catalyzed by diphenyl phosphate has been investigated, which enables the chain propagation reaction to yield the linear oligomers of PCL analogues containing up to 16 mol% of gCCL units. This study contributes to understanding the chemistry of ring-opening reactions of substituted lactones for designing functional degradable polymers.

Received 14th February 2023
Accepted 12th September 2023

DOI: 10.1039/d3ra01025b

rsc.li/rsc-advances

Introduction

Organocatalysts have led to significant progress in organic and polymer syntheses.[1–3] Representative organocatalyzed polymerizations are applicable to ring-opening polymerizations (ROPs) of several heterocyclic monomers such as lactones, cyclic diesters, *O*-carboxyanhyderides, and cyclic carbonates to produce aliphatic carbonyl-containing polymers. These have been extensively studied as biodegradable polymers for a wide range of biomedical applications.[3–5] These biodegradable polymers require additional functionalities, such as cell adhesion properties, enhanced drug loading, and biocompatibility, to fit the applications in regenerative medicine and nanomedicine.[6] Copolymerization and end-modification are often employed to modify and expand the chemical functionalities of these polymers.[7,8] In addition, the preparation of substituted cyclic carbonyl monomers and their ROPs has been explored as a potential route to provide desired functionality to these aliphatic carbonyl polymers.[4,6–8] While extensive efforts have been performed in the literature to introduce different functionalities into degradable polymers, some side-chain structures still affect the polymerizability of the monomers. Depending on the reaction conditions, the ester and amide bonds in the side functional groups have shown some competing mechanisms with the transesterification-based ROPs.[9] In the last two decades, enormous efforts have been addressed to develop organocatalysts, which promote the controlled polymerization of the cyclic esters and carbonates with carbonyl side groups.[5] Alicyclic guanidine and amidine and pairs of thioureas and nitrogen bases have proved controllability and selectivity in the ROPs of these functional monomers, enabling the production of a wide range of side-chain-functionalized biodegradable polymers.[4,5,9]

[a]*Graduate School of Science and Engineering, Yamagata University, Yamagata 992-8510, Japan*
[b]*Graduate School of Organic Materials Science, Yamagata University, 4-3-16 Jonan, Yonezawa, Yamagata 992-8510, Japan*
[c]*POLYMAT, University of the Basque Country UPV/EHU, Joxe Mari Korta Center, Avda. Tolosa 72, 20018 Donostia-San Sebastian, Spain*
[d]*Research Institute for Information Technology, Kyushu University, 744 Motooka, Nishi-ku, Fukuoka 819-0395, Japan*
[e]*Department of Chemistry and Biotechnology, School of Engineering, The University of Tokyo, 7-3-1 Hongo, Bunkyo-ku, Tokyo 113-8656, Japan. E-mail: k_fukushima@chembio.t.u-tokyo.ac.jp*
[f]*Institute for Materials Chemistry and Engineering, Kyushu University, 744 Motooka, Nishi-ku, Fukuoka 819-0395, Japan*
[g]*Japan Science and Technology Agency (JST), PRESTO, 4-1-8 Honcho, Kawaguchi, Saitama 332-0012, Japan*

† Electronic supplementary information (ESI) available. See DOI: https://doi.org/10.1039/d3ra01025b

‡ Takayuki Ota and Valentina Montagna contributed equally to this work.

Poly(ε-caprolactone) (PCL) is a commercially available polylactone with unique elastic properties and has attracted significant attention due to its marine degradable properties.[10,11] In order to enhance the value of these PCL-based polymers, PCL analogues with functional side chains have also been developed.[12–14] These functional PCLs were designed for applications to high-valued biomaterials, such as drug delivery vehicles and tissue engineering scaffolds.[14–16] γ-Carbonyl substituted caprolactones (gCCLs) with an ester linker were first reported by Hedrick and co-workers in 2000, in which they were unable to obtain high-molecular-weight products by the ROP of the gCCLs.[13] Recently, Lang and co-workers reported the successful ROP of gCCLs with amide linker, producing the materials with tunable lower critical solution temperatures[17] Similarly, Stefan and co-workers have recently developed a *tert*-amide linked PCL analogue forming self-assembled nanoparticles.[18]

Synthesis of ester-linked functional PCLs appears still challenging. Nevertheless, this side chain structure remains intriguing for us because of our recent discovery. We have found that functional poly(trimethylene carbonate) (PTMC) analogues with methoxyalkyl ester side chains exhibit excellent antiplatelet properties.[19,20] These results further lead to the recent developments of ether-functionalized PTMC and polydioxanone.[21–23] However, biodegradation of the PTMC analogues proceeds slowly compared to that of aliphatic polyesters.[20,24] We hypothesize that PCL analogues with similar side-chain structures can be of interest because they can indicate different degradation profiles while retaining the blood compatibility.

In this context, we originally designed a CL analogue with 2-methoxyethoxycarbonyl group at the γ-position (**1a**; Fig. 1) to obtain an ether-functionalized PCL analogue by its ROP. However, the desired polymeric product was not formed. Thus, **1b** was prepared as a model compound to elucidate the mechanism of the ring-opening reaction of ester-linked gCCL. In addition, a gCCL **1c** containing an amide linker was examined as another candidate to form the ether-functionalized PCL analogue. These amide-linker types of monomers have shown good polymerizability.[17,18] The present study focuses on understanding the unique reactivity of gCCLs in ring-opening reactions, such as the preference for isomerization into other lactone structures. To this end, we explore several catalysts, including organobases and organoacids (Fig. 1), which have been previously applied in ROPs of cyclic esters and carbonates.[25–29] The most common ROP catalyst stannous 2-ethylhexanoate ($Sn(Oct)_2$) is also examined as a control. Additionally, we demonstrate the copolymerization of gCCL and CL as a pragmatic means to form the ether-functionalized PCL analogue from gCCL.

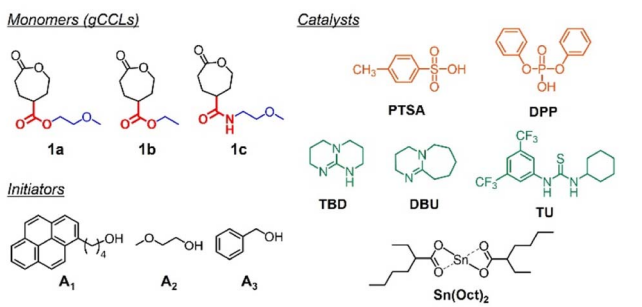

Fig. 1 Chemical structures of γ-carbonyl-substituted ε-caprolactones (gCCLs) **1a–c** (prepared in this study), initiators, and catalysts for ring-opening reactions of the gCCLs. PTSA, *p*-toulenesulfonic acid; DPP, diphenylphosphate; TBD, 1,5,7-triazabicyclo[4.4.0]dec-5-ene; DBU, 1,8-diazabicyclo[5.4.0]undec-7-ene; TU, 1-(3,5-bis(trifluoromethyl)phenyl)-3-cyclohexyl-2-thiourea; $Sn(Oct)_2$, stannous 2-ethylhexanoate.

Results and discussion

Ring-opening reactions of 1a

Target gCCLs **1a–c** were prepared by following the methods reported by Hedrick.[13] Before studying the ROP of **1a**, we evaluated the catalytic activities of the catalysts shown in Fig. 1 toward the ROP of CL. Acidic organocatalysts such as *p*-toluenesulfonic acid (PTSA), and diphenyl phosphate (DPP) exhibited higher catalytic activities than basic 1,5,7-triazabicyclo[4.4.0]dec-5-ene (TBD) (Table S1†). Our preliminary screening also verified that the ROP of CL was faster in toluene than in CH_2Cl_2 (entries 3 *vs.* 4 in Table S1†). Then, we examined the first ring-opening reaction of **1a** (Fig. 2) in toluene (1 M) using DPP (run 1 in Table 1), because this condition achieved a high monomer conversion and narrow molar-mass dispersity in the ROP of CL (entry 3 in Table S1†). The reaction using 1 mol% of 1-pyrenebutanol ($\mathbf{A_1}$) as an initiator was monitored using a ^{1}H NMR, showing the quantitative monomer conversion in 26 h at room temperature (Fig. S1†). The reaction was quenched by adding triethylamine. As with ROP of CL, we tried to precipitate the product in hexane. However, the insoluble fraction was hardly formed. Thus, we analyzed the product using size exclusion chromatography (SEC) by eluting tetrahydrofuran (THF) at 30 °C.

PCL prepared under the same conditions (entry 3 in Table S1†) shows a typical SEC trace characteristic of the polymeric products, appearing at earlier retention time (~20 min) with relatively wide distribution, including a small shoulder around 18 min (Fig. 3). The SEC trace of run 1 in Table 1 indicates a peak A as the major fraction at 28–29 min of the retention time with several small peaks at 24–28 min. Unfortunately, the lower limit of the calibration of the molecular weights was 25 min (Fig. S2a and b†). Thus, reliable molecular weight information (number-average molecular weight: M_n and dispersity: $Đ$) can not be listed, although M_n value of the major fractions (peak A) would be below 1.0×10^3 g mol^{-1} if it could be calibrated. The

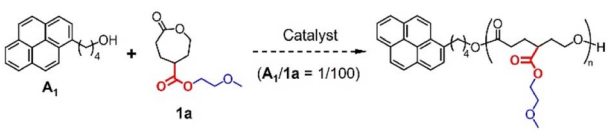

Fig. 2 Desired ring-opening reaction of **1a** using A_1 as an initiator.

Table 1 Ring-opening reactions of **1a** initiated by A_1 in the presence of different catalysts

Run	Catalyst	**1a**/A_1/Cat.	Solvent	[**1a**] (M)	Temperature (°C)	Reaction time (h)	Conversion[a] (%)	Peak A[b] (%)
1[c]	DPP	100/1/1	Toluene	1.0	20–25[d]	26	>99	48
2[c]	DPP	100/1/1	Toluene	1.0	20–25[d]	49	>99	36
3[c]	DPP	100/1/1	CH_2Cl_2	1.0	20–25[d]	27	79	45
4[c]	DPP	100/1/1		Bulk	20–25[d]	29	>99	33
5[e]	TU/DBU	100/1/5/5	Toluene	1.0	20–25[d]	31	>99	41
6[e]	TU/DBU	100/1/5/5	CH_2Cl_2	1.0	20–25[d]	27	>99	63
7	$Sn(Oct)_2$	100/1/1	Toluene	0.5	110	24	32	86
8	$Sn(Oct)_2$	100/1/1		Bulk	110	28	>99	73

[a] Monomer conversion was determined using ^{1}H NMR. [b] Determined from SEC chart (THF, 30 °C) in Fig. 3. [c] The reaction was quenched by triethylamine. [d] Room temperature. [e] The reaction was quenched by benzoic acid.

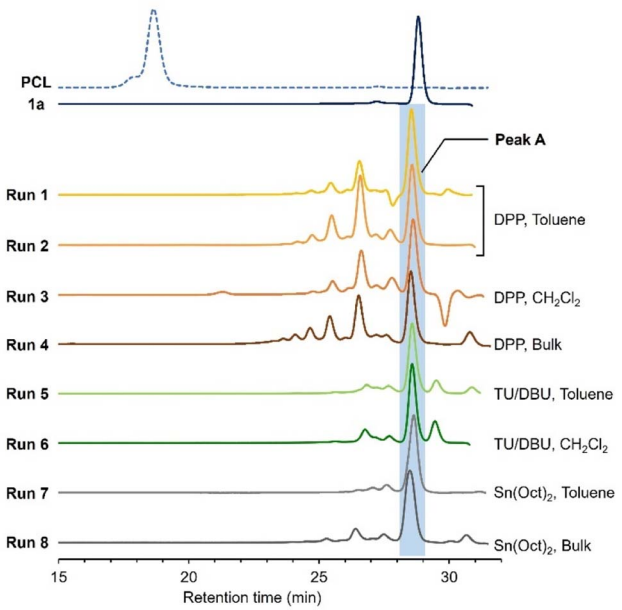

Fig. 3 SEC traces (THF, 30 °C) of the products of the ring-opening reaction of **1a** with A_1 (A_1/**1a** = 1/100) at different runs in Table 1. PCL was prepared by DPP-catalyzed ROP of CL in toluene (entry 3 in Table S1†). Molecular weights were calibrated by polystyrene standards.

peak areas of peak A as the percentage of the major fraction in the reaction product were given in Table 1, instead.

Subsequently, in order to find conditions to obtain the polymeric product as depicted in Fig. 2, we examined the ring-opening reactions of **1a** under different conditions listed in Table 1, that are, varying catalysts, solvents, and temperatures. Strong acids and bases may induce transesterification-based cross-linking and branching, stemming from the side-chain esters. Thus, we employed DPP as a mild acid catalyst[27] and less basic TU/DBU rather than TBD. Since the basic catalyst was found to be less active than acidic ones for the ROP of CL in the preliminary screening and literature,[28] the feed ratios of TU/DBU were increased to 5 mol% (runs 5 and 6 in Table 1). The reaction using $Sn(Oct)_2$ was conducted under heating conditions as it is used in most ROPs[30] (runs 7 and 8 in Table 1). As with the ROP of CL, the DPP-catalyzed reaction proceeded slowly in CH_2Cl_2 (run 3 in Table 1). The $Sn(Oct)_2$-catalyzed reaction in toluene was also slow (run 7 in Table 1). At all runs, the products exhibited similar NMR spectra and SEC traces (Fig. 3). These results suggest the low polymerizability of **1a** and its transformation to some deactivated species with no polymerizability. The ^{1}H NMR spectrum of the reaction mixture of run 1 in Table 1 is different from that expected for the ring-opened structure of **1a** (Fig. S1b†). Accordingly, we suspected a five-membered lactone as a major product of the ring-opening reactions of **1a** (Fig. 4a).

Until a recent study by Chen,[31] five-membered lactones were recognized as non- or low-polymerizable monomers owing to their thermodynamical stability.[12,32] The hydroxy group in the ring-opened species **1a-O** (Fig. 4a) is located four bonds away from the ester carbonyl originally introduced at the γ-position of the CL analogue, which is favorable for the formation of a thermodynamically stable five-membered lactone *via* intramolecular transesterification. Polymerization as an intermolecular reaction (chain propagation in Fig. 4a) is liable to proceed at a high monomer concentration, such as under bulk

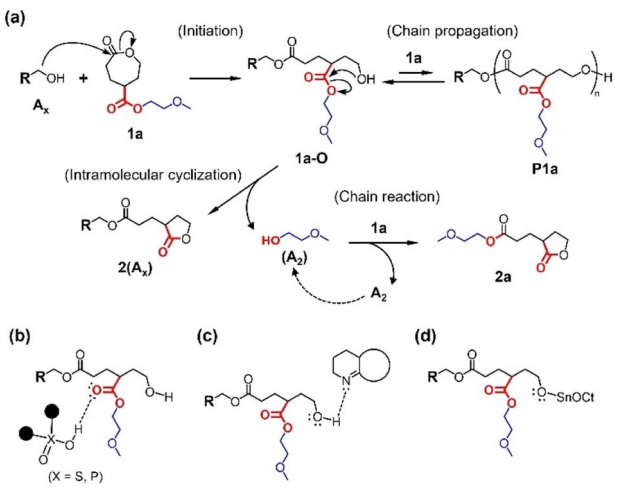

Fig. 4 (a) Plausible formation of five-membered lactones **2**(A_x) and **2a** through a ring-opening reaction of **1a**. (b–d) Plausible activation models of the ring-opened structure **1a-O** by acidic catalysts (b), basic catalysts (c), and $Sn(Oct)_2$.

conditions. However, in the ring-opening reactions of bulk **1a** (runs 4 and 8 in Table 1), no significant differences in the product composition were observed (Fig. 3), suggesting that **1a-O** highly prefers the intramolecular cyclization toward **2(A_x)** in the reaction. The formation of **2(A_x)** involves the release of 2-methoxyethanol (**A_2**) from the side chain of **1a-O**, which serves as a nucleophile to ring-open **1a**. Thus, the chain reaction from **1a** to **2a** is realized (Fig. 4a).

The DPP-catalyzed bulk reaction (run 4 in Table 1) product was further characterized by SEC eluting DMF containing 10 mM LiBr with a refractive index (RI) and ultraviolet (UV) detectors (Fig. S2d†). The SEC trace by a RI detector showed two major peaks: fractions A and B, while that by a UV detector indicated a bimodal peak corresponding to a part of fraction B. Fraction A is UV-undetectable and thus most likely to be **2a**. Since the initiator **A_1** is UV-detectable, fraction B includes the products conjugating **A_1** such as **2(A_1)** and oligomeric **P1a** (Fig. 4a) with **A_1** structure. It should be noted that fraction B contains UV-undetectable products. Considering the feed ratio of **A_1** to **1a** (1/100), the composition of the UV-detectable parts in the whole product should be small. Fraction A also appears to correspond to peak A in the SEC traces in THF (Fig. 3) because its eluted time is close to that of **1a** (Fig. S2c and d†). These results support the formation of **2a** and the chain reaction.

The percentages of peak A in SEC traces of the products in THF vary depending on the catalyst. The DPP-catalyzed reactions (runs 1–4 in Table 1) produced several fractions corresponding to oligomers **P1a** and **2(A_1)** at the retention time between 24 and 28 min (Fig. 3). Thus, the peak A percentages become relatively low (33–48%). The prolonged and concentrated reactions may further facilitate the formation of oligomeric **P1a** and **2(A_1)** *via* transesterification with **2a**, reducing peak A (runs 2 and 4 in Table 1). In contrast, the reaction products using TU/DBU and $Sn(Oct)_2$ predominantly showed peak A (Fig. 3) with high percentages over 60% (runs 6–8 in Table 1), indicating the preferential formation of **2a**. These differences in the product compositions depend on how the ring-opened species **1a-O** is activated by the catalysts (Fig. 4b–d). The DPP-catalyzed ring-opening reaction proceeds through an activated monomer mechanism or a hydrogen-bonding activation pathway, in which the Brønsted acid activates the carbonyl oxygen atom (Fig. 4b).[26,27] Pseudo-anionic mechanism *via* hydrogen-bonding activation is proposed for DBU,[24,28] and coordination–insertion mechanism is believed the most plausible for $Sn(Oct)_2$,[30,33] respectively. The hydroxy oxygen atom of **1a-O** is activated in both DBU- and $Sn(Oct)_2$-catalyzed reactions (Fig. 4c and d).

Based on these activation modes, we performed preliminary density functional theory (DFT) calculations for the model compound of **1a-O** (**1a′-O** in Fig. S3a†). We used the alkoxide anion form (Fig. S3b†) and the oxonium cation form (Fig. S3c†) as the extreme and simplified models of **1a-O** activated by acids and bases/$Sn(Oct)_2$ (Fig. 4b–d). Consequently, the alkoxide anion form immediately yields the intermediate structure of **2**, but the oxonium cation form does not (Fig. S3b and c†). The energy difference between alkoxide anion form and the ring-closed structure in Fig. S3b† was 23.27 kcal mol^{-1}, indicating the stability of the five-membered ring. These results support that the ring-opening reaction products using TU/DBU and $Sn(Oct)_2$ contain high percentages of peak A (Table 1). Accordingly, the organobasic catalysts are preferred over the organoacidic ones for the formation of five-membered lactones. In addition, the results of the DFT calculations also indicate that the intramolecular cyclization occurs in a geometry-dependent manner as the six-membered lactone is not favorably formed from the analogue of **1a-O** with additional methylene between the ester group and OH (Fig. S3d†). Our result is consistent with the previous quantum chemical calculation, which revealed the high stability of the five-membered ring of γ-butyrolactone compared to the six-membered ring of δ-valerolactone.[32]

Subsequently, we performed an equimolar reaction of **1a** with **A_2** to verify whether **1a-O** (R = CH_2OCH_3) or **2a** could be obtained. In this reaction, TU/DBU (5% each relative to **1a**) were used as the catalysts to obtain products with low contents of oligomers. The reaction was completed in 4.5 h, and the crude reaction product was almost a single component (Fig. S4a†). The crude product was purified by column chromatography using ethyl acetate : hexane of 1 : 1 and silica gels. The purified product was then characterized using NMR and Fourier-transform infrared (FT-IR) spectroscopies to verify the formation of **2a** (Fig. 5 and S5–S7†). The integral ratios in the ^1H NMR spectrum matched those of the structure of the five-membered lactone **2a** rather than those of the linear ring-opened structure

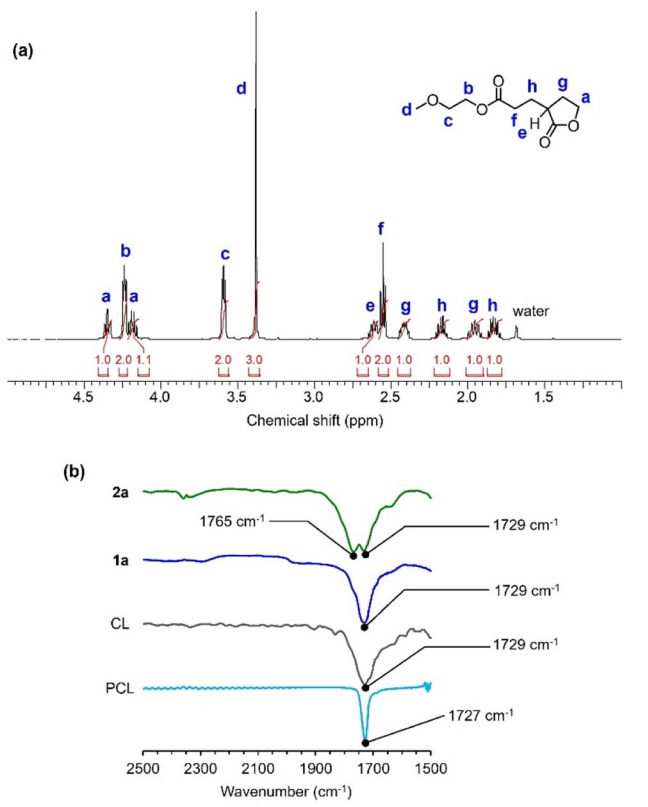

Fig. 5 Spectroscopic characterization of **2a**. (a) Expanded region of ^1H NMR (500 MHz) spectrum of **2a** in $CDCl_3$. (b) Expanded region of FT-IR spectra of the C=O stretching bands in **2a**, **1a**, CL, and PCL.

of **1a-O** (Fig. 5a). In addition, the FT-IR spectrum of **2a** exhibited the characteristic peaks of the five-membered-ring-strained and linear esters at 1765 and 1729 cm^{-1}, respectively (Fig. 5b). The crude reaction product exhibited a similar ^1H NMR spectrum (Fig. S4a†) to that showed in Fig. 5a and S4b,† indicating instability of **1a-O** in the reaction mixture. These observations verify the preferential formation of the five-membered lactone through intramolecular transesterification.

Ring-opening reactions of 1b with equimolar alcohols

The equimolar ring-opening reaction further invoked our interest regarding equilibrium between the five-membered lactone and the released alcohol (Fig. 6). Thus, we examined the equimolar ring-opening reaction of **1**, using different alcohols $\mathbf{A}_x$, solvents, and catalysts. Compound **1b** was additionally synthesized and used because its simple structure is beneficial for spectroscopic characterizations and it is simply derived from a commercially available material in one reaction.

Different ring-opening reactions with DPP, TU/DBU, and $Sn(Oct)_2$ as catalysts were conducted. These three catalysts were used in the ring-opening reactions of **1a** (Table 1) and thus selected as the representatives of organoacids, organobases, and organometallic catalysts. The purpose for conducting these reactions was to verify whether the released alcohol (ethanol) can compete with the initiator alcohol reagent ($\mathbf{A}_x$) to form mixed five-membered lactones **2b** and **2($\mathbf{A}_x$)** and whether the competition depends on the catalytic mechanism and solvent (Fig. 6). The selective formation of a five-membered lactone depending on the catalyst and solvent was also verified. The DPP-catalyzed reactions produced a single component when $\mathbf{A}_1$ was used as the initiator (run 1 in Table 2 and Fig. S8a†). This is because **2($\mathbf{A}_1$)** was insoluble in toluene and precipitated once formed, avoiding competing with the released ethanol in the reaction. The products of the reactions in toluene using $\mathbf{A}_2$ and $\mathbf{A}_3$ (runs 2 and 3 in Table 2, Fig. S8b and c†) were the mixtures of **2b** and **2($\mathbf{A}_x$)** (1 : 1). These results may explain the low percentages of peak A at runs 2 and 4 in Table 1 as a result of transesterification between **2($\mathbf{A}_1$)** and **2a** (Fig. 4). The reaction with initiator $\mathbf{A}_3$ in $CHCl_3$ preferably yielded **2b** with 97% of selectivity (run 4 in Table 2). Furthermore, when DBU/TU and $Sn(Oct)_2$ were used as catalysts (runs 5–8 in Table 2 and Fig. S8d†), the same reactions yielded only **2b**, irrespective of solvents.

DPP acts as a Lewis acid and activates the carbonyl groups through hydrogen bonding, facilitating the nucleophilic attack by the hydroxy group of ring-opened **1b** and $\mathbf{A}_x$. For the ring-opening reaction in toluene, the hydrogen-bonding activation by DPP is sufficiently effective for not only the lactone carbonyl of **1b** but also for the linear ester of **2($\mathbf{A}_x$)** to form **2b**, reaching the equilibrium (runs 2 and 3 in Table 2). The predominant formation of **2b** in the reactions using $\mathbf{A}_3$ (runs 4–8 in Table 2) suggests that the released benzyl alcohol ($\mathbf{A}_3$) is not involved in the substitution of the ethyl ester of **2b**. It should be noted that the basicity of ethanol and benzyl alcohol is close (pK_a in water: 15 *vs.* 14).[34] Polarity of $CHCl_3$ may enhance this slight difference in the basicity of these alcohols as nucleophilicity when DPP is used (run 4 in Table 2). In contrast, the activation of the alcohol hydroxy groups by TU/DBU and $Sn(Oct)_2$ may differentiate their nucleophilicity over the effects of solvent polarity (runs 5–8 in Table 2). We may propose these ring-opening reactions as a way of selectively forming functional five-membered lactones, which are potentially used as precursors and building blocks of high-value chemicals and medicines,[35,36] by selecting appropriate solvents and catalysts.

Table 2 Ring-opening reactions of **1b** with different catalysts and equimolar alcohols $\mathbf{A}_x$

Run[a]	Alcohol	Catalyst	Loading[b] (equiv.)	Solvent	**2($\mathbf{A}_x$) : 2b**[c]
1	$\mathbf{A}_1$	DPP	0.1	Toluene	100 : 0
2	$\mathbf{A}_2$	DPP	0.1	Toluene	55 : 45
3	$\mathbf{A}_3$	DPP	0.1	Toluene	55 : 45
4	$\mathbf{A}_3$	DPP	0.1	$CHCl_3$	3 : 97
5	$\mathbf{A}_3$	TU/DBU	0.02, 0.02	Toluene	0 : 100
6	$\mathbf{A}_3$	TU/DBU	0.02, 0.02	$CHCl_3$	0 : 100
7	$\mathbf{A}_3$	$Sn(Oct)_2$	0.02, 0.02	Toluene	0: 100
8	$\mathbf{A}_3$	$Sn(Oct)_2$	0.02, 0.02	$CHCl_3$	0 : 100

[a] All reactions were conducted for 1 h at 20–25 °C (room temperature). [b] Relative to **1b**. [c] Determined using ^1H NMR.

Ring-opening reactions of 1c

The formation of ester bonds through alcoholysis of amide is thermodynamically unfavorable. Thus, we expect to obtain PCL analogues without the formation of five-membered lactones by ROP of **1c** containing the 2-methoxyethyl substituent linked through an amide bond (Fig. 7). The ring-opening reactions of **1c** with different catalysts were examined and compared with those of **1a**. It should be noted that these experiments are performed to find the conditions to obtain the polymeric product from **1c**, not to evaluate catalytic activities and reaction rate. The monomer-initiator ratios were the same as the reactions of **1a** (**1c**/$\mathbf{A}_x$ = 100/1). Compared to the reactions of **1a** that were mostly completed in approximately 30 h, longer reaction times

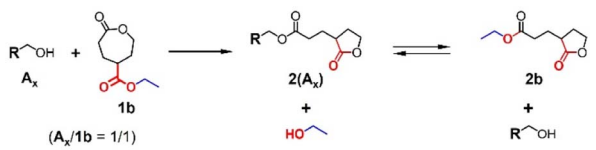

Fig. 6 Equimolar ring-opening reaction of **1b** using alcohols $\mathbf{A}_x$ as initiators.

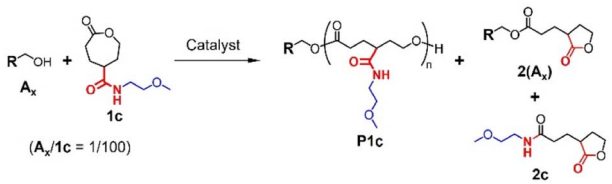

Fig. 7 Ring-opening reaction of **1c** and the estimated products.

and heating (90, 100 °C) were required for high conversion of **1c** (Table 3). This is partially attributable to the poor solubility of **1c** in toluene. Although CH_2Cl_2 shows better solubility for **1c**, it is not an appropriate solvent for the heating reactions due to its low boiling point.

The incomplete monomer conversions were observed in several conditions. The DPP-catalyzed reaction with the catalyst loading of 1 mol% did not proceed. The DPP-loading was then stepwise increased up to 15 mol% to finally reach the monomer conversion of 57% for 77 h (run 1 in Table 3). Acidic catalysts are often used for the polymerization of monomers with acidic protons, such as amide NH.[25,37] However, in this study, the monomer conversion appeared to stop at a certain time after loading of DPP, suggesting the catalyst deactivation by some byproducts. TBD also did not start the reaction with 1 mol% of the loading, which increased to 5 mol% to convert 77% of **1c** slowly taking 152 h (run 2 in Table 3). $Sn(Oct)_2$-catalyzed reactions facilitated high monomer conversions (runs 3 and 4 in Table 3 and Fig. S9†). Accordingly, no catalysts provided explicit polymeric products (**P1c** in Fig. 7) as major products under several temperatures and concentrations.

The SEC traces of the products were similar to those of the ring-opening reactions of **1a**, in which the major fractions are eluted at late retention times (29–31 min; Fig. 8a). The percentages of the major fractions vary by catalysts. The reactions catalyzed by DPP and TBD produced the major fractions over 60% (runs 1 and 2 in Table 3). The $Sn(Oct)_2$-catalyzed reactions yielded lower percentages of the major fractions (<41%; runs 3 and 4 in Table 3) with a larger area of sub-peaks at 26–28 min, suggesting more formation of oligomers. Similar results were observed in a previous report by Lang,[17] which demonstrated the successful formation of several PCL analogues with amide side groups at the γ-position but a less hindered residue. The FT-IR spectra of the reaction products exhibit the characteristic C=O stretching band around 1766 cm^{-1} (Fig. 8b), suggesting the formation of the five-membered lactone ring, such as **2(A_x)** and **2c** (Fig. 7). Thus, we need to consider the intramolecular cyclization through alcoholysis of the amide side chain (Fig. S10†), which is unusual and rarely observed.

The reaction pathways of the ring-opening reactions of **1c** are different from those of **1a**. Achieving 100% monomer conversion in the reactions of **1c** was difficult, particularly when using acidic catalysts. This is probably attributed to the behavior of 2-metxhoyethylamine (2MEA) released as a byproduct during the formation of the five-membered lactone **2(A_x)** from the ring-opened species **1c-O** (Fig. S10†), forming salts or adducts with the acidic catalysts. The released 2MEA in the reaction of **1c** can be involved in the ring-opening reaction of another **1c**, leading to the chain reaction for the formation of **2c** (Fig. S10†). However, the linear ester structure was remained in the products of the TBD- and $Sn(Oct)_2$-catalyzed reactions (Fig. 8b). These results suggest that both the five-membered lactone and the ring-opened species are present in the equilibrium (Fig. S10†), differently from the case of **1a**. Accordingly, the reaction products of **1c** included complex structures (Fig. 7).

The equimolar reactions of **1c** with benzyl alcohol (**A_3**) were studied to understand the mechanism of the ring-opening reaction of **1c** in a simpler manner. The equimolar ring-

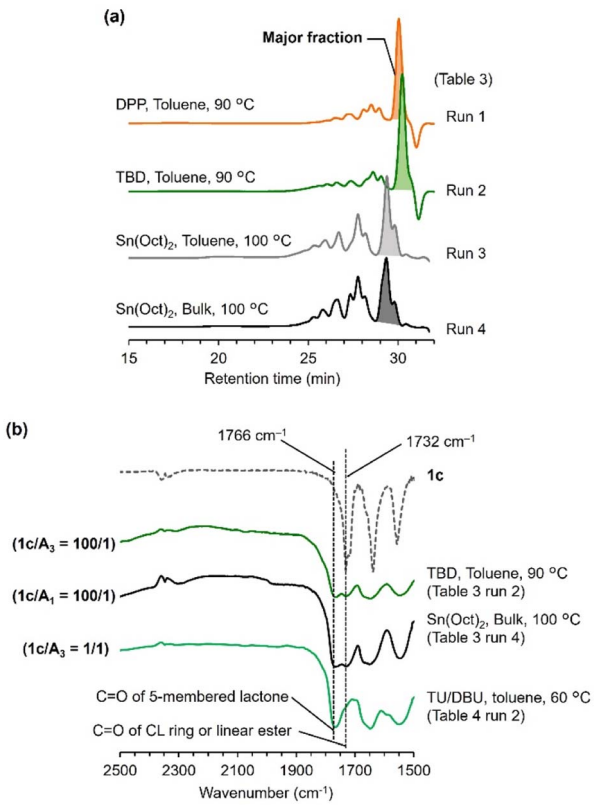

Fig. 8 Characterization of the products of the ring-opening reactions of **1c**: (a) SEC traces (THF, 30 °C) and (b) expanded regions of FT-IR spectra.

Table 3 Ring-opening reactions of **1c** with different catalysts

Run	Initiator	Catalyst	**1c**/A_x/Cat.	Solvent	[**1c**] (M)	Temperature (°C)	Time (h)	Conversion[a] (%)	Major fraction[b] (%)
1	**A_3**	DPP	100/1/1–15[c]	Toluene	1.0	90	77	57	66
2	**A_3**	TBD	100/1/1–5[d]	Toluene	1.0	90	152	77	60
3	**A_1**	$Sn(Oct)_2$	100/1/1	Toluene	1.0	100	36	>99	41
4	**A_1**	$Sn(Oct)_2$	100/1/1.5	Bulk		100	73	80	38

[a] Determined using ^{1}H NMR. [b] Determined from SEC chart in Fig. 8a (THF, 30 °C). [c] DPP is gradually loaded up to 15 mol%. [d] TBD is added in the middle of the reaction to be 5 mol%.

opening reaction of **1c** was not completed in the presence of 0.1 equiv. of DPP (Fig. S11†). The increased loading of DPP by 1.0 equiv. resulted in full conversion of **1c** (run 1 in Table 4). The product exhibited a characteristic signal for benzyl ester at 5.2 ppm and no signal around 5.9 ppm for amide NH in the ^{1}H NMR spectrum (Fig. S11†), suggesting the predominant formation of **2(A$_3$)** (Fig. S10†). These results rationalize our assumption that the released amine forms an adduct with DPP, not attacking **2(A$_3$)** to form **2c**. In contrast, the reactions catalyzed by basic organocatalysts DBU in the presence of a co-catalyst TU (run 2 in Table 4) proceeds in a different manner. The time course of the reaction mixture in the presence of TU/DBU monitored by ^{1}H NMR (Fig. S12†) suggested that the reaction product at 2 h contained **2(A$_3$)** and **1c-O** (Fig. S10†), which were eventually transformed into **2c** at 24 h. In the NMR spectra, the reaction product at 2 h shows the distinct signal for benzyl ester at 5.2 ppm, which completely disappears at 24 h (Fig. S12†). Instead, the sharp and single signal for amide NH at 5.9 ppm emerges at 24 h, reminding us of the reaction between **2(A$_3$)** and the released 2MEA. These results indicate that 2MEA is active in the TU/DBU-catalyzed reaction of **1c**, forming **2c**. The low conversion of **1c** in the reaction using water as the initiator indicates that a carboxyl group is formed on the ring-opened species **1c-O** (RCH$_2$ = H; Fig. S10†) to mitigate the basic catalyst (run 3 in Table 4).

Copolymerization of 1a and CL

The DPP-catalyzed ring-opening reactions of **1a** provided more oligomeric products than those catalyzed by TU/DBU and Sn(Oct)$_2$ (Fig. 3). Based on our analyses of various reactions mentioned earlier, reactions with acidic catalysts and at room temperature are preferable for mitigating intramolecular cyclization. In addition, incorporating other monomer units that do not induce internal cyclization would facilitate chain propagation to form a linear polymer structure. Therefore, we studied the DPP-catalyzed ring-opening copolymerization of **1a** and CL in toluene at room temperature using **A$_1$** as the initiator (Fig. 9a). Two **1a**/CL feed ratios of 10/90 and 25/75 were used for the reactions. All monomers were consumed for 31 h, as confirmed by ^{1}H NNR. After precipitation in a 1 : 1 mixture of hexane and methanol, precipitated products were obtained. The SEC traces of the precipitates exhibited explicit broad peaks corresponding to polymeric products, although distinguished sharp peaks suggesting the presence of **2a** were also confirmed

Table 4 Ring-opening reactions of **1c** using equimolar benzyl alcohol (A$_3$) and water as initiators

Run[a]	Initiator	Catalysts	Loading (equiv.)	[**1c**] (M)	Time (h)	Conv. (%)
1	**A$_3$**	DPP	0.1–1.0[b]	0.2		>99
2	**A$_3$**	TU/DBU	0.2, 0.2	0.7	3	>99
3	H$_2$O	TU/DBU	0.1, 0.1	0.6	24	28

[a] All reactions were conducted in toluene at 60 °C. [b] Gradually increased to 1.0 equiv.

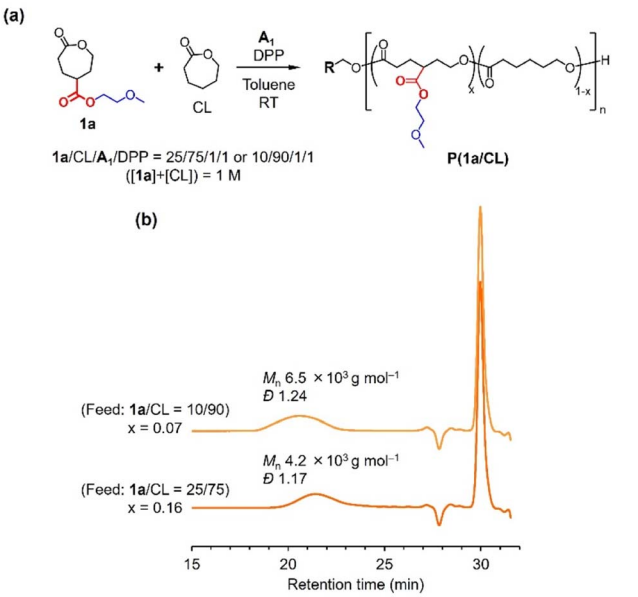

Fig. 9 Ring-opening copolymerization of **1a** and CL: (a) synthetic scheme, (b) SEC traces of the copolymerization products (THF, 30 °C, PS standards).

(Fig. 9b). The calibrated M_ns of the copolymerization products were 6.5 and 4.2 × 10^3 g mol^{-1}, respectively. The dispersities ($Đ = M_w/M_n$) were relatively narrow, indicating the low degrees of chain transfer and transesterification in the DPP-catalyzed copolymerization. The ^{1}H NMR spectra of the products (Fig. S13†) suggested the successful incorporation of **1a** in PCL, imparting the compositions of **1a** (x) in the copolymers as 0.07 and 0.16. The comonomer ratios in the copolymers of **1a** and CL (**1a**/CL = 7/93 and 16/84) corresponded well with the original feeding ratios (10/90 and 25/75), proving that polymerization proceeded in a controlled manner. Although a five-membered lactone structure may be formed at the copolymer chain end, several emerging signals on the NMR spectra (Fig. S13†) confirm the successful formation of the ether-functional PCL analogues.

Conclusions

We investigated ring-opening reactions of three types of γ-substituted ε-caprolactones with the substituents linked by ester and amide bonds, using different organocatalysts. A five-membered lactone was preferentially formed in all reactions compared to the functionalized PCL analogues. Detailed studies revealed that the hydroxy groups located four bonds away from the ester carbonyl group at the ring-opened structure of gCCLs readily induced intramolecular cyclization *via* transesterification. The compositions of the ring-opening reaction products of gCCLs depend on the catalysts used. Basic organocatalysts facilitate the formation of five-membered lactones **2(A$_x$)**, while acidic organocatalysts provide more fractions of linear oligomeric products. Thus, DPP-catalyzed copolymerization of CL and **1a** successfully provided PCL analogues bearing

methoxyethyl ester side chains with molecular weights of several thousands. In this study, the five-membered lactone was also preferentially formed from a γ-amide-substituted CL, suggesting the significance of the steric effect in intramolecular alcoholytic cyclization with cleavage of the amide bond. The results of the present work will be further used in designing on-demand degradable polymers, where the equilibrium in aminolysis of five-membered lactones is engineered. In addition, our findings can be applied to prepare substituted five-membered lactones, which can be potentially used as precursors of medicines and high-value chemicals.

Conflicts of interest

There are no conflicts to declare.

Acknowledgements

This work was supported by JSPS KAKENHI (JP25870078, JP18K12074, JP19H05715, JP19H05716, JP19H05718, and JP19H05720), JST PRESTO (JPMJPR21N7), JST COI (JPMJCE1312), Izumi Science and Technology Foundation (H24-J-129), and Iketani Science and Technology Foundation (0301087-A). The authors are grateful to Prof. Hideharu Mori of Yamagata University for the assistance of the SEC measurements. The authors would like to thank Editage for the English language editing.

Notes and references

1 J. Seayad and B. List, *Org. Biomol. Chem.*, 2005, **3**, 719–724.
2 S. Shirakawa and K. Maruoka, *Angew. Chem., Int. Ed.*, 2013, **52**, 4312–4348.
3 N. E. Kamber, W. Jeong, R. M. Waymouth, R. C. Pratt, B. G. G. Lohmeijer and J. L. Hedrick, *Chem. Rev.*, 2007, **107**, 5813–5840.
4 K. Fukushima, *Polym. J.*, 2016, **48**, 1103–1114.
5 W. N. Ottou, H. Sardon, D. Mecerreyes, J. Vignolle and D. Taton, *Prog. Polym. Sci.*, 2016, **56**, 64–115.
6 K. Fukushima, *Biomater. Sci.*, 2016, **4**, 9–24.
7 W. Yu, E. Maynard, V. Chiaradia, M. C. Arno and A. P. Dove, *Chem. Rev.*, 2021, **121**, 10865–10907.
8 Y. Yu, J. Zou and C. Cheng, *Polym. Chem.*, 2014, **5**, 5854–5872.
9 K. Fukushima, ROP of Cyclic Carbonates, in *Organic Catalysis for Polymerisation*, eds., A. P. Dove, H. Sardon and S. Naumann, Royal Society of Chemistry, Cambridge, 2019, ch. 7, pp. 274–327.
10 M. Suzuki, Y. Tachibana and K. Kasuya, *Polym. J.*, 2021, **53**, 47–66.
11 G.-X. Wang, D. Huang, J.-H. Ji, C. Völker and F. R. Wurm, *Adv. Sci.*, 2021, **8**, 2001121.
12 K. Fukushima and T. Fujiwara, New Routes to Tailor-Made Polyesters, in *Polymers for Biomedicine*, ed., C. Scholz, John Wiley & Sons, Inc., Hoboken NJ, 2017, ch. 6, pp. 149–190.
13 M. Trollsås, V. Y. Lee, D. Mecerreyes, P. Löwenhielm, M. Möller, R. D. Miller and J. L. Hedrick, *Macromolecules*, 2000, **33**, 4619–4627.
14 E. A. Rainbolt, K. E. Washington, M. C. Biewer and M. C. Stefan, *Polym. Chem.*, 2015, **6**, 2369–2381.
15 E. M. Pelegri-O'Day, S. J. Paluck and H. D. Maynard, *J. Am. Chem. Soc.*, 2017, **139**, 1145–1154.
16 M. E. Prévôt, H. Andro, S. L. M. Alexander, S. Ustunel, C. Zhu, Z. Nikolov, S. T. Rafferty, M. T. Brannum, B. Kinsel, L. T. J. Korley, E. J. Freeman, J. A. McDonough, R. J. Clements and E. Hegmann, *Soft Matter*, 2018, **14**, 354–360.
17 L. Wen, S. Zhang, Y. Xiao, J. He, S. Zhu, J. Zhang, Z. Wu and M. Lang, *Macromolecules*, 2020, **53**, 5096–5104.
18 E. L. Calubaquib, P. Soltantabar, H. Wang, H. Shin, A. Flores, M. C. Biewer and M. C. Stefan, *Polym. Chem.*, 2021, **12**, 3544–3550.
19 Y. Watanabe, S. Takaoka, Y. Haga, K. Kishi, S. Hakozaki, A. Narumi, T. Kato, M. Tanaka and K. Fukushima, *Polym. Chem.*, 2022, **13**, 5193–5199.
20 K. Fukushima, Y. Inoue, Y. Haga, T. Ota, K. Honda, C. Sato and M. Tanaka, *Biomacromolecules*, 2017, **18**, 3834–3843.
21 V. Montagna, J. Takahashi, M.-Y. Tsai, T. Ota, N. Zivic, S. Kawaguchi, T. Kato, M. Tanaka, H. Sardon and K. Fukushima, *ACS Biomater. Sci. Eng.*, 2021, **7**, 472–481.
22 Y. Watanabe, R. Kato, K. Fukushima and T. Kato, *Macromolecules*, 2022, **55**, 10285–10293.
23 K. Fukushima, Y. Ota and T. Kato, *Macromol. Chem. Phys.*, 2022, **223**, 2200192.
24 R. P. Brannigan and A. P. Dove, *Biomater. Sci.*, 2017, **5**, 9–21.
25 K. Fukushima and K. Nozaki, *Macromolecules*, 2020, **53**, 5018–5022.
26 D. J. Coady, H. W. Horn, G. O. Jones, H. Sardon, A. C. Engler, R. M. Waymouth, J. E. Rice, Y. Y. Yang and J. L. Hedrick, *ACS Macro Lett.*, 2013, **2**, 306–312.
27 K. Makiguchi, T. Satoh and T. Kakuchi, *Macromolecules*, 2011, **44**, 1999–2005.
28 R. C. Pratt, B. G. G. Lohmeijer, D. A. Long, R. M. Waymouth and J. L. Hedrick, *J. Am. Chem. Soc.*, 2006, **128**, 4556–4557.
29 B. G. G. Lohmeijer, R. C. Pratt, F. Leibfarth, J. W. Logan, D. A. Long, A. P. Dove, F. Nederberg, J. Choi, C. Wade, R. M. Waymouth and J. L. Hedrick, *Macromolecules*, 2006, **39**, 8574–8583.
30 A. Kowalski, A. Duda and S. Penczek, *Macromolecules*, 2000, **33**, 689–695.
31 M. Hong and E. Y.-X. Chen, *Nat. Chem.*, 2016, **8**, 42–49.
32 K. N. Houk, A. Jabbari, H. K. Hall and C. Alemán, *J. Org. Chem.*, 2008, **73**, 2674–2678.
33 A. Kowalski, A. Duda and S. Penczek, *Macromolecules*, 2000, **33**, 7359–7370.
34 A. Hellqvist, Y. Hedeland and C. Pettersson, *Electrophoresis*, 2013, **34**, 3252–3259.
35 G.-H. Pan, R.-J. Song and J.-H. Li, *Org. Chem. Front.*, 2018, **5**, 179–183.
36 S. Gupta, R. Arora, N. Sinha, M. I. Alama and M. A. Haider, *RSC Adv.*, 2016, **6**, 12932–12942.
37 K. Fukushima, K. Matsuzaki, M. Oji, Y. Higuchi, G. Watanabe, Y. Suzuki, M. Kikuchi, N. Fujimura, N. Shimokawa, H. Ito, T. Kato, S. Kawaguchi and M. Tanaka, *Macromolecules*, 2022, **55**, 15–25.